P- and S-wave migration of while drilling data

G. Bernasconi

Dipartimento di Elettronica e Informazione, Politecnico di Milano, Italy

(Received: March 28, 2007; accepted: November 21, 2007)

ABSTRACT I investigate some aspects of multicomponent processing in seismic while drilling (SWD) acquisitions. I start from the consideration that a working roller cone is a good source of both P- and S-waves. Then, by examining the radiation pattern of the bit, I evaluate the subsurface illumination in simple models and for different geophone directivity. Results show that S-waves can increase the lateral extent of the imaged area, while P-waves achieve a higher illumination in the vicinity of the borehole. By using the appropriate velocity model, it is possible to obtain a migrated gather for P-waves and one for S-waves separately. In addition, migration gathers can be observed in the aperture angle domain. Results on SWD synthetic data confirm this analysis. I also produce P- and S-wave migrated gathers from field data: their comparison reveals the presence of a coherent signal for the two wave modes. The information thus collected about both compressional and shear properties of the subsurface, especially during the drilling process, can be crucial to predicting overpressured zones and to reducing the ambiguity between variations in pore pressure and variations in lithology.

1. Introduction

Overpressured zones present significant challenges for optimizing the drilling process. Knowledge of pore pressure using seismic data, as for instance from seismic-while-drilling techniques (SWD), will help producers plan the drilling in real time to control potentially dangerous abnormal pressures. Many authors have addressed the problem of pore pressure prediction from seismic data (Carcione and Gangi, 2000; Bowers, 2002; Freitag *et al*., 2004). An important observation is that ambiguities exist between variations in pore pressure and variations in lithology and fluid content. Multicomponent data provides both compressional and shear information and can resolve or at least reduce these ambiguities (Sayers *et al*., 2001).

I investigate the processing of compressional and shear waves in SWD acquisitions when using tricone bits. Theoretical studies and laboratory experiments (Sheppard and Lesage, 1988; Rector and Hardage, 1992) show that tricone bits generate both compressional and shear waves during the drilling process. The authors of these studies have also produced radiation patterns of the drill-bit for the different waves. I use these radiation patterns in simple subsurface models in order to analyze the illumination of the medium around the borehole, both in the spatial coordinates (depth and offset from the borehole), as well as in the angular coordinate (aperture angle between incident and reflected rays on a target). This analysis shows that due to the directivity of the source (bit) and of the receivers (geophones on the surface), P- and S-waves are complementary: the combined use of compressional and shear waves can increase the extension of the imaged area and, where both waves are present, can strengthen the identification of rock parameters.

© 2008 – OGS

I generate synthetic data for SWD acquisition geometries, modeling the bit radiation pattern and the geophone directivity, and I show the results of migration when using the P- and the S-velocity models. Again, the migrated gathers can be used together to improve the interpretation.

I also show results on real 3D SWD data.

2. Radiation pattern of a tricone bit

Rector and Hardage (1992) model the tricone drill-bit signal as a pseudo random series of bit-tooth impacts that create both axial forces and tangential torques around the borehole axis. P-waves radiate primarily along the axis of the borehole, and S-waves radiate primarily perpendicular to the borehole axis. So, in a vertical hole, the largest P-waves will be recorded directly above and below the bit, whereas the largest shear waves will be recorded in a horizontal plane containing the drill bit. In a deviated well, the radiation patterns should be rotated by the inclination angle of the drill bit. The authors find that this theoretical modeling is confirmed by field data examples. I start from their result, which assumes that the seismic radiation pattern, generated by the axial drill-teeth impacts on the rock, can be modeled as a transient monopolar point force $g(t)$ acting along the axis of the borehole. So, the far field displacements are

$$U_r(r,\phi,t) = \frac{A\cos\phi}{\rho V_P{}^2 r} g\left(t - \frac{r}{V_P}\right), \tag{1}$$

$$U_\phi(r,\phi,t) = \frac{A\sin\phi}{\rho V_S{}^2 r} g\left(t - \frac{r}{V_S}\right), \tag{2}$$

where ρ is the medium density, r is the distance from the source (bit) to the wavefront, V_P and V_S are the compressional and shear velocity of the medium, A is a scalar, ϕ is the angle relative to the borehole axis. U_r is the radial displacement (P-waves). U_ϕ represents SV-motion since the particle displacement is in a plane containing the borehole axis and perpendicular to U_r. Fig. 1 shows the far-field wave amplitude distribution corresponding to Eqs. (1) and (2). The relative amplitudes of the P- and SV-radiation lobes are determined by the Poisson ratio of the formation being drilled. Results show that a working bit is a good source of SV-wave energy: for typical Poisson ratio values, SV-wave displacements are larger than P-wave displacements.

Transverse drill-bit impacts occur in synchronization with axial impacts. They are responsible for the generation of SH-waves. Laboratory measurements (Sheppard and Lesage, 1988) show that the magnitude of the transverse forces are significantly lower than the magnitudes of the axial forces. For typical tricone drill conditions the SH displacements are approximately three orders of magnitude lower than the SV displacements (Rector and Hardage, 1992), and they will be neglected in this paper.

3. Subsurface and angular illumination

As a preliminary example, I consider a vertical drilling well in an isotropic model with a single

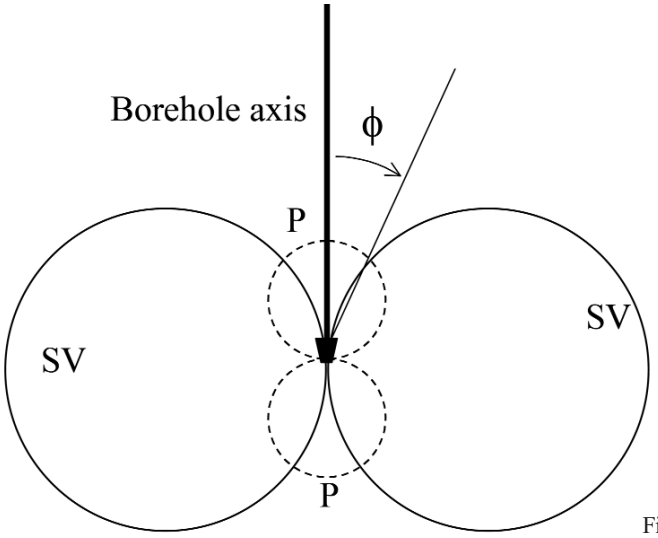

Fig. 1 - Radiation pattern of a roller-cone drill bit.

horizontal reflector, 1800 m deep. I compute synthetic data arriving at surface receivers from sources (bit levels) spanning the vertical borehole from 400 m to 1700 m. Vertical and horizontal geophones are arranged along a line intersecting the well, with offset ranging from –4000 m to 4000 m. Geophone spacing is 25 m. Medium velocities are V_P=2500 m/s and V_S=1760 m/s. The model is drawn in Fig. 2a. Using multicomponent geophones, due to the directivity of the source, we mainly obtain P-wave events on the near offset vertical geophones, and S-wave events on the far offset horizontal geophones. Fig. 2 shows some synthetic data: common shot (bit) gathers (Figs. 2b and 2c) and common receiver gathers (Figs. 2d and 2e). The main events are the direct arrivals of P- and S-waves and the primary P-P and SV-SV reflections. For sake of simplicity I have neglected mode conversions and other waves that are present in SWD acquisitions, such as the tube waves departing from the drill string, and the surface waves departing from the rig structure. As I am interested in the subsurface illumination, I have also by-passed the processing steps necessary to obtain RVSP-like seismic traces, that is the correlation with an estimated source signature, deconvolution by the drill-string response, delay corrections (Poletto and Miranda, 2004).

Fig. 3a shows an illumination map of the subsurface for P-waves. Fig. 3b is the illumination map for SV-waves. These maps are produced, for each depth point, by summing the contributions of sources and receivers, corrected by their directivity. The directivity of the source is the radiation pattern of the bit, the directivity of the receiver is the angular response of the geophone. Darker zones correspond to higher illumination. In presence of noise, the accuracy of the subsurface imaging is directly linked to the illumination. Comparison of the maps reveals that P- and S-waves are complementary: P-waves mainly enlighten the area around the well while S-waves cover higher offsets. This can be exploited to increase the lateral extension of the investigated area. However, a portion of the subsurface is illuminated by the two waves: in this case multicomponent analysis provides additional information for the prediction of media parameters.

I have migrated the synthetic SWD data with a Kirchhoff depth migration code (Bernasconi, 2002), using the P- and S-velocity models. The results are shown in Fig. 4. The reflector depth is

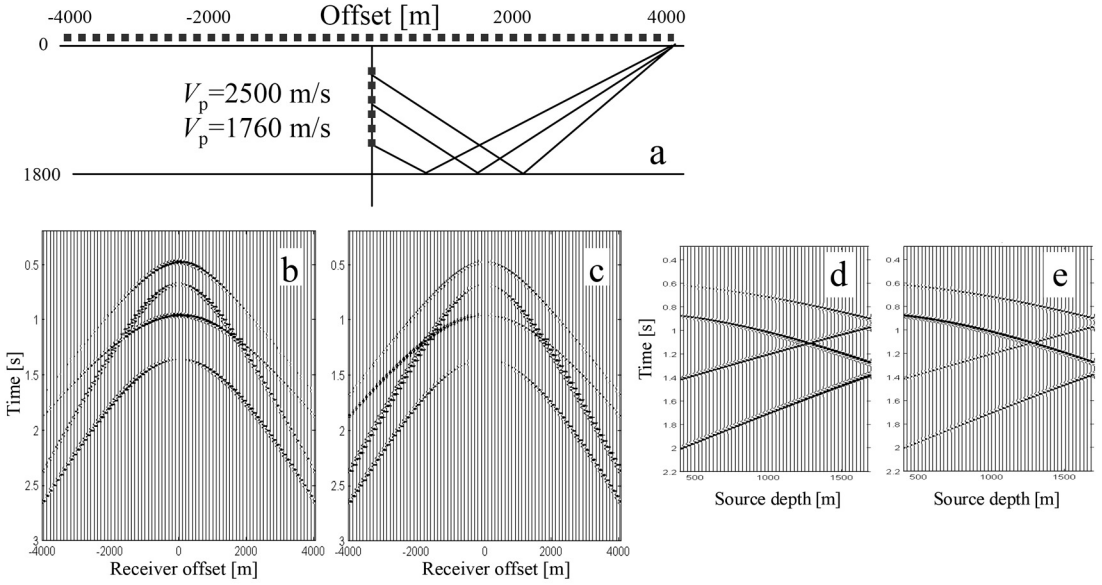

Fig. 2 - Model for the generation of synthetic SWD data (a). Dotted lines indicate the position of sources (bit levels) and receivers. Common shot gathers (bit depth 1200m): vertical geophones (b) and horizontal geophones (c). Common receiver gathers (offset 1500 m): vertical geophones (d) and horizontal geophones (e).

correctly recovered, but the different illumination of compressional and shear waves is still evident. In fact, the migration of vertical geophones, using the P-velocity model (Fig. 4a), recovers a portion of the reflector near the well. The migration of horizontal geophones, using the S-velocity model (Fig. 4b), recovers a portion of the reflector away from the well. As expected, the resolution for S-waves is higher than the one for P-waves.

I have also analyzed the aperture angle coverage on the reflector at different distances from the well, by computing migrated aperture angle gathers (Vassallo and Bernasconi, 2004). Figs. 4c and 4d

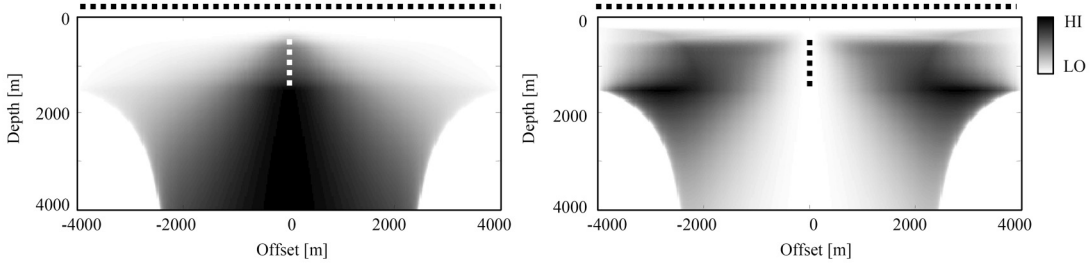

Fig. 3 - Subsurface illumination (model in Fig. 2): P-waves and vertical geophones (a), SV waves and horizontal geophones (b). Dotted lines indicate the position of sources (bit) and receivers.

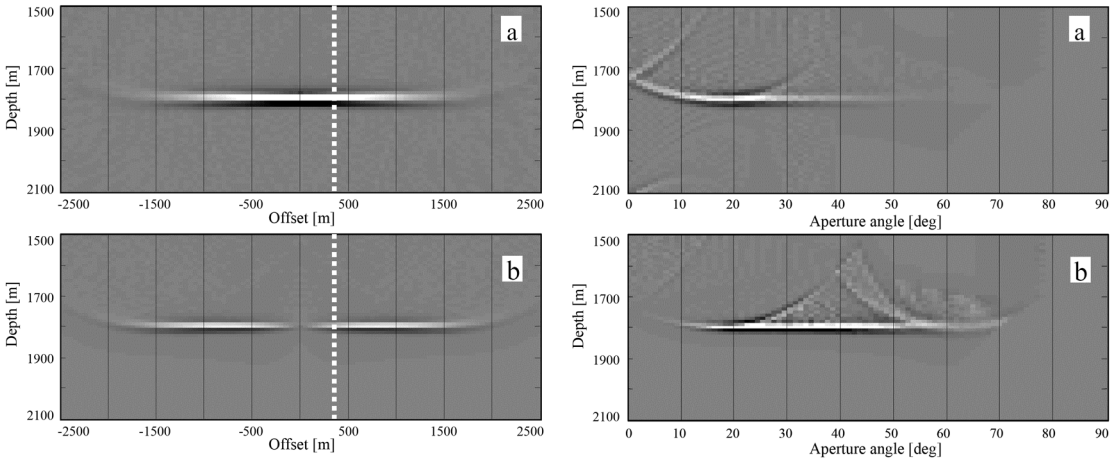

Fig. 4 - Depth migrated gathers (model in Fig. 2): vertical geophones with P-velocity model (a), horizontal geophones with S-velocity model (b). Aperture angle gathers for offset 300 m (dotted line in the depth migrated gathers): vertical geophones with P-velocity model (c), horizontal geophones with S-velocity model (d).

are angle gathers for the horizontal offset position of 300 m. Vertical axis is depth, horizontal axis is aperture angle between incident and reflected rays at the depth point. I have applied a control on the migrated dips in order to reduce migration artifacts (Bernasconi, 2002): in this case, the maximum absolute migrated dip has been limited to 30°. The aperture angle coverage is different for P-waves (Fig. 4c) and for S-waves (Fig. 4d). P-waves enlighten small aperture angles (< 30°), S-waves reach higher values and lack small apertures. The amplitude along the angle direction, provided we are compensating the propagation and illumination effects (true amplitude migration), is proportional to the reflection coefficient versus angle. The estimation of both P-P (from the P gather) and SV-SV (from the S gather) reflection coefficients is of primary importance to determine the media parameters that generate the seismic event.

4. 1D medium example

Now, I consider a more complex example, simulating a vertical well drilled in a horizontally layered medium (Fig. 5). The model parameters (P-velocity V_P, S-velocity V_S and density ρ) are obtained from a real well log. I compute synthetic seismograms arriving at surface receivers from 133 sources (bit levels) spanning the vertical borehole from 430 m to 3070 m. Source spacing is 20 m. Vertical and horizontal geophones are arranged along a line, with offset ranging from 25 m to 5000 m. Geophone spacing is 25 m. Synthetic traces are computed with the reflectivity method (Muller, 1985): they contain direct arrivals, reflections, conversions, multiples. The source is a vertical single force that models the tricone bit directivity. Fig. 6 is a common receiver gather, at a near offset from the well (250 m). Due to the direction of arrival of the waves radiated by the bit, P-waves are predominant in the vertical component (Fig. 6a) and S-waves are predominant in the horizontal component (Fig. 6b). At larger offsets, this wavefield separation is less pronounced: it is important to take into account the fact that shear waves are present also in the vertical geophones and

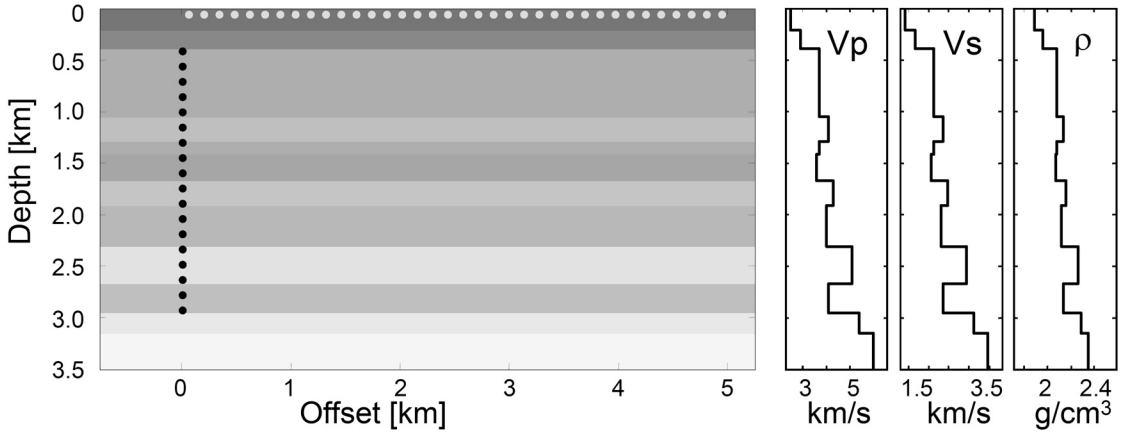

Fig. 5 - 1D model for the computation of synthetic traces. Dotted lines are the position of sources (bit) and receivers.

compressional waves are visible also in the horizontal geophones. This consideration will be recalled in the real data example, where only vertical geophones are available.

I have migrated the synthetic data, separately for vertical and horizontal components, on the P- and S-velocity model. No wave separation has been applied: the focusing or defocusing of events is committed totally to the migration summation. Fig. 7 is the result for all possible combinations. When using the P-velocity model and the vertical component, only the P-waves will add constructively to the correct position (Fig. 7a). On the other hand, when using the S-velocity model

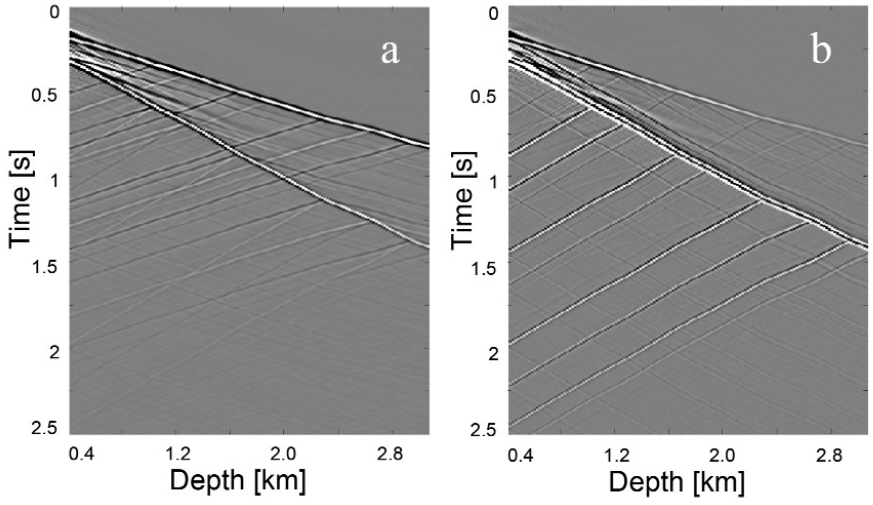

Fig. 6 - Synthetic data for the model in Fig. 5. Common receiver gather, offset position 250 m: vertical component (a), horizontal component (b)

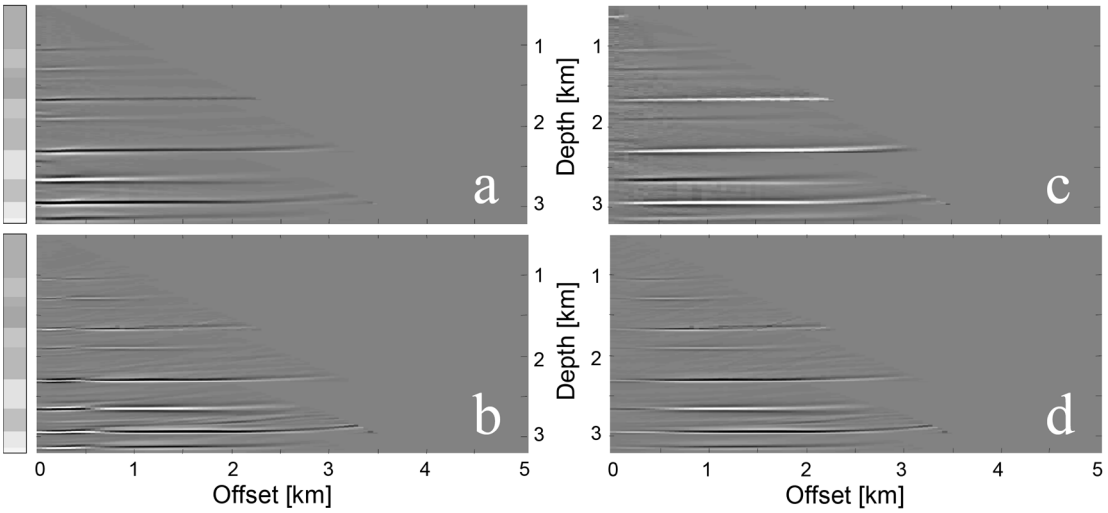

Fig. 7 - Depth migration, model in Fig. 5: P waves on vertical geophones (a), S waves on horizontal geophones (b), P waves on horizontal geophones (c), S waves on vertical geophones (d). On the left the position of the layers.

and the horizontal component, the S-waves will image the reflectors at the correct position (Fig. 7b). Figs. 7c and 7d demonstrate that shear waves are also present in the vertical geophones and compressional waves are present in the horizontal geophones. All the gathers show a good and accurate reconstruction of the reflectors. There are also some noise and some "phantom" horizons, for example in Fig. 7a, at near offsets and at a depth of around 2.5 km, or in Fig. 7b, at a depth of around 2.75 km. They are due to multiples, conversions and "unwanted" reflections (S-waves when using P-velocity or P-waves when using P-velocity) that do not interfere destructively in the summation, or accidentally sum up in phases at certain positions of the subsurface.

It is interesting to note a polarity change in the reflectors when imaged with the S-waves, produced by a change of sign in the reflection/transmission coefficient of some interfaces. Again, S-waves achieve a better resolution with respect to P-waves.

Fig. 8 shows aperture angle gathers for the horizontal offset position of 500 m. The vertical axis is depth, the horizontal axis is the aperture angle between incident and reflected rays at the depth point. The angular coverage is slightly different for P- and S-waves. Non-horizontal events are linked to multiples, conversions and reflections that are not focused with the velocity model (P or S) used in the migration: they are attenuated by the summation along the aperture angle dimension. In this example, unfocused events show up particularly in P-wave records (Figs. 8a and 8c), but it depends on the offset and on the relative amplitudes of reflections and conversions. Furthermore, unfocused events are imaged in different regions of the subsurface (also outside the target zone), depending on the velocity model used by the migration.

The analysis presented here for simple models can be done for deviated wells and in more complex velocity models by rotating the radiation pattern of the source and by properly computing the Green functions between depth points and sources/receivers.

For PDC bits, the different radiation pattern has to be taken into account (Poletto and Miranda, 2004).

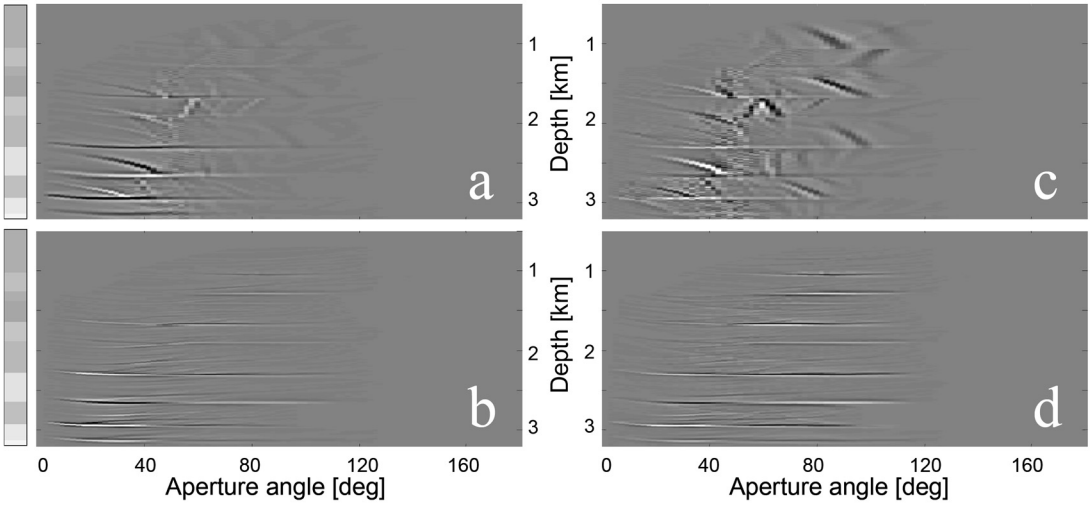

Fig. 8 - Depth migration, model in Fig. 5. Aperture angle gathers for offset 500 m: P waves on vertical geophones (a), S waves on horizontal geophones (b), P waves on horizontal geophones (c), S waves on vertical geophones (d). Position of the layers on the left.

5. Field data example

The field data set was acquired by ENI and OGS (Bertelli *et al*., 1998; Poletto *et al*., 2001). Surface receivers are set down along two orthogonal lines crossing at the well and along two circles centered on the well. The internal circle has a radius of approximately 1100 m and the external circle has a radius of 2200 m. The saw-tooth shaped circular disposition facilitates the separation of the surface arrivals (noise) from the deep arrivals (signal from the bit). The total number of receivers is

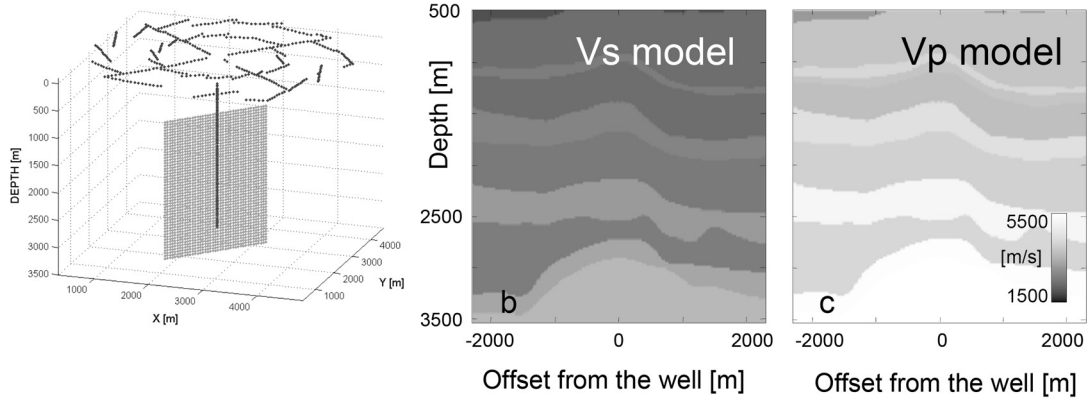

Fig. 9 - 3D SWD acquisition and velocity model. Acquisition geometry and position of the migrated target (a). Velocity models (b, c) refer to the target.

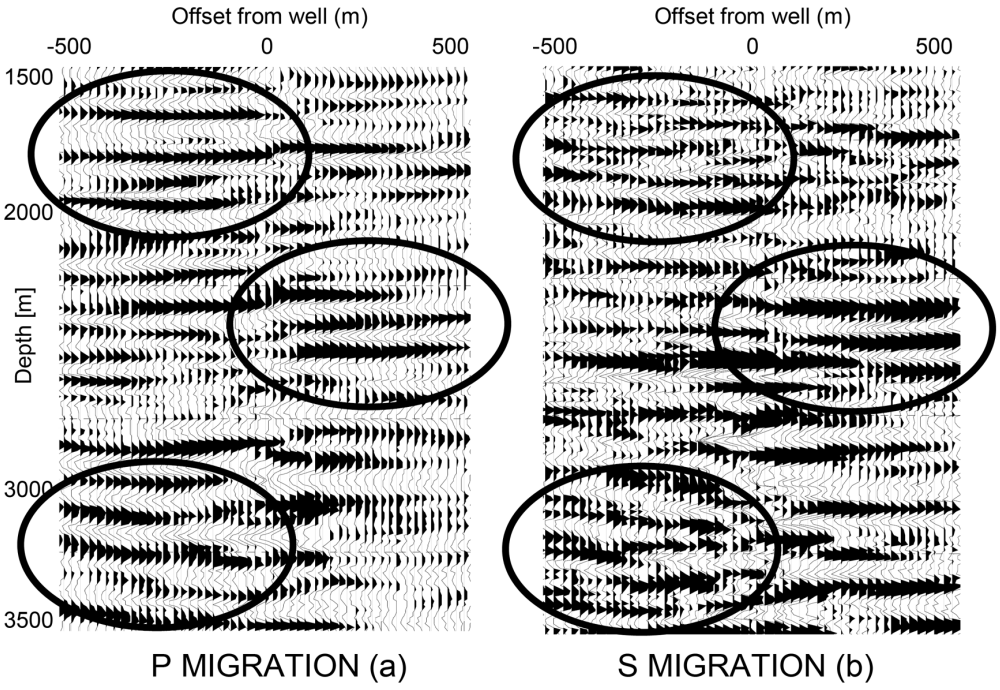

Fig. 10 - Migration of 3D SWD real data. P-waves with P-velocity model (a), and S-waves with S-velocity model (b). Circled areas highlight similarities.

391. The acquisition starts at a depth of 428 m to a depth of 3060 m, for a total count of 166 levels. ENI and OGS provided the processed data (equivalent RVSP survey) and the 3D P- and S-velocity models.

I consider a vertical target slice of 1000 m in the horizontal direction and 2000 m in the vertical direction, centered around the well. Fig. 9 shows the acquisition geometry and the velocity models in the target. Only vertical geophones are available. I have run two migrations, one with the P-velocity model and one with the S-velocity model. In the first case, focusing of P-waves is predominant, in the second case, the shear waves (projected along the vertical direction) mainly sum up the model constructively. Fig. 10a is the migration of P-waves, with the P-velocity model. Fig. 10b is the migration of S-waves with the S-velocity model. The two images have a similar "trend" and this is an indicator of the presence of a coherent signal for the two wave modes. There is also a good correlation in many parts of the target: circled areas highlight similarities. S-wave image exhibits a slightly higher resolution and an increased "far offset" coverage, especially for the positive offsets. This is not so evident for negative offsets, probably due to near surface conditions.

6. Conclusions

Tricone bits are a good source for both compressional and shear waves. These waves can be recorded during the perforation and they can be processed in order to gain information about the rock

properties. I have shown that, due to the directivity of the bit, P- and S-waves produce a different illumination of the subsurface. This information can be exploited to increase the total imaged area around the borehole. I have migrated synthetic and real SWD data with the P- and S-velocity model. The summation process helps the separation of compressional and shear waves and it is possible to build two images of the migrated target. So, the additional information provided by the S-waves may improve the reliability of overpressure and media parameter prediction.

Acknowledgements. I thank ENI and OGS for providing the real data set and Massimiliano Vassallo for help in the migration process.

REFERENCES

Bernasconi G.; 2002: *Kirchhoff depth migration of 3D SWD data.* EAGE Internat. Mtg, Expanded Abstracts.

Bertelli L., Miranda F., Poletto F. and Rocca F.; 1998: *Design of SWD 3D RVSP using Seisbit® technology.* Extended Abstracts, EAGE Internat. Mtg., Paper 10-49.

Bowers G.L.; 2002: *Detecting high overpressure*. The Leading Edge, **21**, 174-177

Carcione J.M. and Gangi A.F.; 2000: *Gas generation and overpressure: effects on seismic attributes.* Geophysics, **65**, 1769–1779.

Freitag H.C., Kirkwood A. and Reese M.; 2004: *An enhanced approach to real-time pore pressure prediction for optimized pressure management while drilling*. The Leading Edge, **23**, 574-578.

Muller G.; 1985: *The reflectivity method: a tutorial.* Journal of Geophysics, **58**, 153-174.

Poletto F. and Miranda F.; 2004: *Seismic While Drilling, Fundamentals of Drill-Bit Seismic for Exploration*. Handbook of Geophysical Exploration, Seismic Exploration, Vol. 35, Elsevier.

Poletto F., Miranda F., Petronio L., Bertell L., Malusa M., Luca A. and Schleifer A.; 2001: *3D RVSP drill-bit survey – Preliminary results*. Extended Abstracts, EAGE Internat. Mtg., Paper M12.

Rector J. W. and Hardage B. A.; 1992: *Radiation pattern and seismic waves generated by a working roller-cone drill bit*. Geophysics, **57**, 1319-1333.

Sayers C.M., Woodward M.J. and Bartman R.C.; 2001: *Predrill pore-pressure prediction using 4-C seismic data.* The Leading Edge, **20**, 1056-1059.

Sheppard M.C. and Lesage M.; 1988: *The forces at the teeth of a drilling roller-cone bit: theory and experiment*. SPE Paper 18042.

Vassallo M. and Bernasconi G.; 2004: *SWD data migration with regularization of illumination in the angle domain*. EAGE Internat. Mtg, Expanded Abstracts.

Corresponding author: Giancarlo Bernasconi
Dip. di Elettronica e Informazione
Politecnico di Milano
P.zza Leonardo da Vinci 32, 20133 Milano, Italy
phone: +39 02 23993453; fax: +39 02 23993413; e-mail: bernasco@elet.polimi.it